2022-08

A review of thermal impact of surface acoustic waves on microlitre droplets in medical applications

Mehmood, M

http://hdl.handle.net/10026.1/19584

A review of thermal impact of surface acoustic waves on microlitre droplets in medical applications

Mubbashar Mehmood[1,2], Umar F Khan[3], Ali OM Maka[4], Javed Akhter[5] , Tariq Nawaz Chaudhary[6] , Faisal Masood[7], Sameer Ahmad Hasan[8] and Yeaw Chu Lee[9]

Abstract

The surface acoustic waves (SAW) propagate inside the microdroplets resulting in kinetic and thermal impacts. The kinetic drives fluid particles inside the droplet while thermal impact increases the liquid's temperature. This paper provides a comprehensive review of the research investigations related to internal kinetics and heating inside the microdroplet caused by the acoustic waves. The main factors that affect the kinetics and convection heat transfer are the piezoelectric materials, shape of the interdigital transducer (IDT) and mode of acoustic waves. Internal streaming (kinetic) leads to particle mixing, particle manipulation, cell sorting, cell patterning, cell separation, measuring the concentration of immunoglobulin and so forth. The effect of changing the mode of waves and the shape of IDT on the relevant applications are presented. Internal convection heat transfer is important where heating of the liquid is essential for many applications such as monitoring blood coagulation in the human plasma and an acoustic tweezer for particle trapping. Experimental methods developed by researchers to realise uniform temperature with constant heating and cooling cycles are also discussed. Such methods are widely used in the polymerase chain reaction (PCR) to detect COVID-19 infection. The heating of the droplet can be efficiently controlled by changing the input power and by varying the duty factor.

Keywords

Surface acoustic wave (SAW), droplet microfluidics, acoustothermal, piezoelectric material, temperature control, polymerase chain reaction (PCR)

[1]School of Engineering and Physical Sciences, Heriot-Watt University, Edinburgh, UK
[2]Department of Mechanical Engineering, National University of Technology, Islamabad, Pakistan
[3]Department of Computer Science, EdgeHill University, Ormskirk, Lancashire, UK
[4]The Libyan Centre for Research and Development of Saharian Communities, Mourzuq, Libya
[5]Faculty of Mechanical and Aeronautical Engineering, University of Engineering and Technology Taxila, Rawalpindi, Pakistan
[6]Department of Mechanical Engineering, University of Engineering and Technology Lahore, Pakistan
[7]Department of Electrical Engineering, University of Engineering and Technology Taxila, Rawalpindi, Pakistan
[8]Department of Biomedical Engineering, German Jordanian University, Jordan, Amman, Jordan
[9]School of Engineering, Computing and Mathematics, Faculty of Science and Engineering, University of Plymouth, Devon, UK

Corresponding author:
Javed Akhter, Department of Mechanical Engineering, University of Engineering and Technology Taxila, Rawalpindi 47080, Pakistan.
Email: javed.akhter@uettaxila.edu.pk

Introduction

The acoustic waves have many applications in communication, sensing, actuation, quantum system, mesoscopic and biological systems.[1] The acoustic waves are mainly classified as surface generated acoustic waves (SGAWs) and bulk acoustic waves (BAWs).[2–4] SGAWs include surface acoustic waves (SAW), Pseudo surface acoustic waves (PSAW) and Leaky surface acoustic waves (LSAW). Bulk acoustic waves include shear bulk acoustic waves (S-BAW), longitudinal bulk acoustic waves (L-BAW), film bulk acoustic waves (FBAR) and Lamb waves. SAWs have further four modes, named Rayleigh surface acoustic waves, Sezawa, Shear-horizontal surface acoustic waves and Love waves.[5]

Common thin-film materials used for SAW generation mainly include quartz (SiO_2), cadmium sulphide (CdS), zinc oxide (ZnO), gallium arsenide (GaAs), aluminium nitride (AlN), lithium tantalate ($LiTaO_3$) (LT), lithium tetraborate ($Li_2B_4O_7$), lithium niobate ($LiNbO_3$) (LN), langasite ($La_3Ga_5SiO_{12}$) and lead zirconate titanate ($Pb(Zr,Ti)O_3$) (PZT).[6,7] Although, quartz is often employed in precision sensing because of its low temperature coefficient of frequency, which leads to good thermal stability, piezoelectric materials such as LN, LT and PZT have substantially greater coefficients of electromechanical coupling, therefore making them extremely viable for SAW-based applications.[8] However, LN and LT suffer from poor control of film stoichiometry, orientation, texture and process parameters[9–12] whereas PZT films are quite difficult to fabricate.[13] Nonetheless, the use of thin-film piezoelectric materials can be easily combined with lab-on-a-chip (LOC) and microfluidic devices at a relatively low cost while enabling the combination of multiple functions on varied substrates. In addition, these piezoelectric films can be selectively deposited in places where an acoustic wave is needed, simplifying design of SAW device by preventing contact between the active layer and the liquid droplet.

The liquid droplets are manipulated through kinetic processes such as micro-mixing, pumping, jetting, nebulisation, and deformation under the influence of SAW.[14–19] On the other hand, thermal impact of SAW on the liquid droplets include heating and evaporation of the droplets which is very important for LOC and microfluidic applications.[20–24] Keeping in view the importance of these facets, many research investigations have been conducted during the past few decades and it has recently gained greater attention of the researchers to evaluate its various aspects. Therefore, it makes imperative to review the previous literature related to thermal and kinetic impacts of SAW on micro droplets with special emphasis on their medical applications.

The present study mainly focuses on the review of recent developments of SAW generation with the use of basic IDT structures that examine how changing SAW modes and IDT designs can affect the kinetic and thermal impacts of microlitre droplets. The knowledge related to the generation of waves, material required, and their applications has been summarised. The review articles are available for streaming, mixing, jetting, nebulisation, pumping etc. However, a comprehensive review is required for how the kinetics can be linked with the convection heat transfer caused by the waves inside the droplet, which is crucial for LOC and other biomedical applications. Section 1 presents general introduction and need for this review while section 2 describes kinetic inside the microlitre droplets followed by section 3 which illustrates heating of the droplet. Section 4 describes medical applications of the waves and section 5 concludes the article with future recommendations.

Kinetics inside the droplet

The movement of particles inside the droplet or movement of the entire liquid droplet is known as kinetics. Recent advances in acoustofluidics have enabled kinetic processes such as mixing, pumping, jetting and nebulisation, that has numerous applications in biochemical analysis, disease diagnosis, and drug delivery.[25–27]

Generation of surface acoustic waves

A wave of a few hundred MHz with nanometre-scale amplitudes can be easily generated using an IDT.[28] Providing an alternating current (AC) or radio frequency (RF) to the electrodes of the IDT fabricated on the piezoelectric material generates acoustic waves due to piezoelectric effect. These waves travel along the surface of the material, that's why called as surface acoustic waves.[28]

IDT designs can vary in shape and configuration to facilitate relevant applications. Different types of IDTs and the most common applications related to each IDT are shown in Figure 1. When IDTs are arranged such that the generated waves are directed towards the centre of the IDT is called focussed IDT (FIDT).[29] Alternatively, this configuration can be circular (circular IDT) to provide focussed acoustic pressure and energy to generate the desired pumping and mixing in microfluidics, which produces high droplet velocities and concentration effects.[30] On another side, slanted IDT designs, also known as tapered IDT have electrodes tapered from one side to the other, can be employed to guide and control the direction and movement of droplets by continuously altering its operating
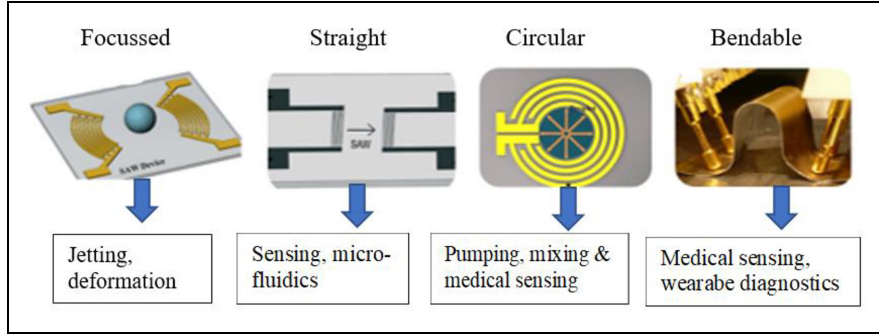
Figure 1. Different designs of IDT devices and their relevant applications. [29,31,37–39]
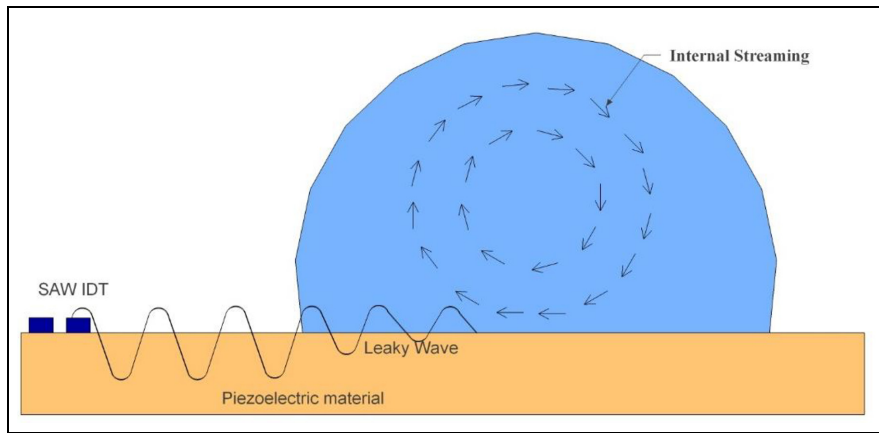

Figure 2. SAW-droplet interaction, IDT fabricated on the piezoelectric material.

frequency.[31] IDTs fabricated on flexible substrate piezoelectric material can be employed as flexible IDTs. Such devices are typically used in different medical applications including medicine delivery, wearable diagnostics and surgical treatments.[32–37]

In this section, various types of IDTs and their relevant applications are summarised. The next section introduces how streaming generates inside the fluid using surface acoustic waves.

Streaming inside microdroplet

Acoustic streaming is the phenomenon caused by radiation forces inside liquid droplets absorbing high-frequency acoustic oscillations as shown in Figure 2.[40] At low radio frequency (RF) power values, streaming and internal mixing has been observed. Conversely, at higher power values, effect may induce droplet deformation or subsequent displacement that moves it from one place to another.[41] Therefore, SAW is responsible for generating acoustic radiation pressure (P) inside the liquid droplet[7] that can be determined by using the relation given in equation (1)[7]:

$$P = \rho_o V_s^2 \left(\frac{\Delta\rho}{\rho_o} \right)^2 \qquad (1)$$

where ρ_o is density of the fluid, V_s is the velocity of sound in the solid while $\Delta\rho$ represents change in their densities. Figure 2 illustrates SAW-droplet interaction, droplet is placed on the piezoelectric material where waves generate internal streaming in the droplet.

Capillary waves are another type of acoustic waves which are generated at the liquid-air interface when leaky wave propagates inside the liquid droplet. If sufficiently high SAW power is provided during this process, the acoustic pressure dominates the surface tension and capillary stress. As a result it begins to destabilise the interface which subsequently cause deformation, jetting, nebulisation.[17,18,42,43]

SAW modes are characterised by using the ratio of substrate thickness, h, and acoustic wavelength, λ. If the ratio is greater than one ($\frac{h}{\lambda} > 1$), Rayleigh mode waves are observed and if it is less than one ($\frac{h}{\lambda} < 1$), Lamb mode waves are generated.[38] In the case when $\frac{h}{\lambda} \approx 1$, a surface reflected bulk wave (SRBW), or hybrid wave, is generated[27] and is a combination of both Rayleigh and Lamb waves. Devices which use these
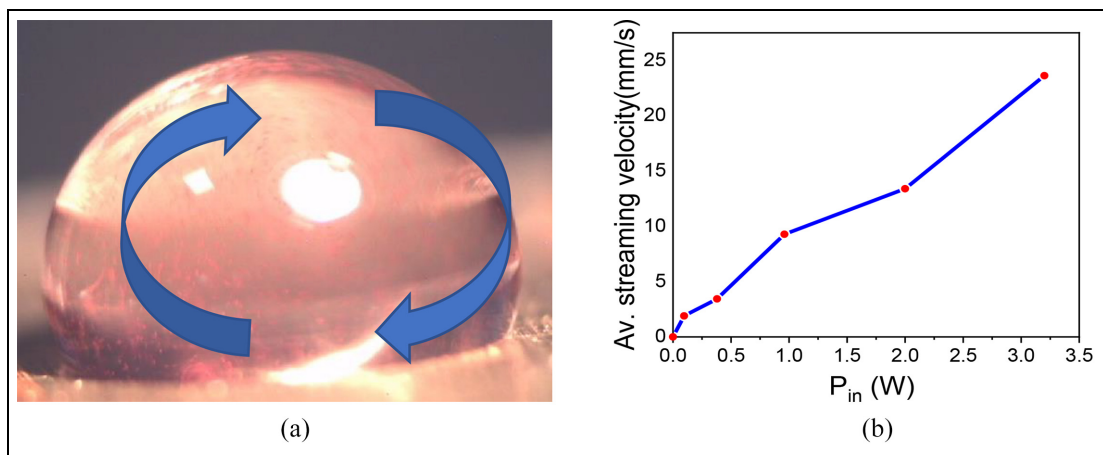
Figure 3. Streaming inside 25 µl water droplet with 6 µm polystyrene particles (a) side view and (b) streaming velocity of particles against various input power levels.[51]

waves are called hybrid resonant acoustics (HYDRA) devices which are primarily used for nebulisation of the droplet and where both sensing and actuation is required with the same device.[27,44]

Many SAW devices are based on Rayleigh oscillatory modes and are most commonly used in microfluidics.[45] Rayleigh surface acoustic waves (RSAW), which consist of both longitudinal and vertical shear components, create waves which move along the substrate's surface. These are generated on bulk piezoelectric substrates with specified orientations, such as ST-cut and Y-cut quartz, X-112° Y-cut LT and 128° Y-X-cut LN[46] substrates.[47] R-SAW can also be generated using vertically aligned thin films of zinc oxide, aluminium nitride, PZT and lithium niobate on (0002) oriented plane.[13,48] In both configurations, its acoustic energy rapidly decays into the material leading to excessive damping. Higher modes of R-SAW in layered substrates generate Sezawa and Kanai modes and propagate on the surface when the thin film's acoustic wave velocities are much smaller than those within the substrate or sub-layer beneath.[49] Notably, this makes the temperature sensitivity and temperature co-efficient of frequency (TCF) of Sezawa waves 1.6 to 1.8 times higher than R-SAW.[50] On the other hand, shear dominated waves such as SH-SAW, made from quartz, 36° Y-X-cut *LN* and 64° Y-X-cut LN,[13] and Love mode waves that transpire in SH-SAW, whose surface is covered with a thin waveguide layer (such as quartz or zinc oxide) to entrap the generated waves, are suitable for applications where sensitivity is required.

Using R-SAW with resonant frequency of 26.300 MHz (wave velocity of 2630 m/s) with ZnO thin film placed on an aluminium plate IDT device, streaming velocity inside a droplet has been estimated as low as 2 mm/s using an input power of 96 mW for a 25 µl water droplet. To visualise streaming inside the droplet,

particles of size 6 µm have been used and tracking takes place using particle image velocimetry (PIV) as shown in Figure 3. The side view of the droplet has been presented in Figure 3(a) with incident waves originating from the left and the particles move from bottom to top in a clockwise direction as indicated by the arrow. Figure 3(b) delineates the corresponding near-linear increase in droplet streaming velocities, showing the rate of 5.0 mm/s/W as observed from 1.0 to 2.0 W.[51]

Lamb waves are either Bulk acoustic waves or surface generated acoustic waves. These are generated from the substrate having thickness less than or equal to the wavelength of the waves.[13] Passive Lamb waves are generated from remote source of acoustic waves without using piezoelectric material as substrate. However, positive Lamb waves can be generated using thin piezoelectric substrate layer.[13] The type of substrate material and its thickness have direct effect on the performance of the Lamb waves.[52] The IDT material required for generation of these waves may include Al_2O_3/PZT that has enhanced performance and reduced dispersiveness of the waves.[53] Common propagation modes of these waves are zero-order symmetrical mode (S_0) and zero-order anti-symmetric mode (A_0).[13,54] A_0 mode is also known as flexural plate waves (FPW), that has enhanced applications in mixing and pumping.[55] In comparison, S_0 wave mode's energy is relatively small and has applications in liquid sensing.[13,56] In the case when a pair of IDTs is used, the acoustic input applied from both sides produces standing surface acoustic waves (SSAW)[57] which are useful in many applications such as jetting, focussing, patterning, particle manipulation, and separation.[13,58]

The Love waves are generated by covering the substrate's surface with a thin film of materials such as ZnO, TeO_2 or polymers. These waves have high sensitivity and are not suitable for microfluidic

Table 1. Types of waves, their potential applications and limitations.

Type of waves	Substrate material	Applications	Problems/limitations	References
SSAW	128° X-propagation LiNbO$_3$	Particle's separation, manipulation, and patterning	Can be only used in microchannel or microchamber	Shi et al.[57], Yeo and Friend[58]
BAW-FBAR	-	Low power consumption, small size and high sensitivity	Not good for microfluidic applications because of high fabrication cost, large noise/signal ratio	Fu et al.[13]
Lamb waves	ZnO with Aluminium foil	A_0 mode has applications in mixing and pumping while S_0 mode is ideal for sensing	A_0 mode is not efficient as compared to Rayleigh mode whereas S_0 mode has low potential for microfluidic applications	Grate et al.[54], Lamb[61], Muralt et al.[62]
SH-SAW	36° YX-cut LiNbO$_3$ and 64° YX-cut LiNbO$_3$	Better performance in sensitivity detection, low cost, low power consumption	Not good for microfluidic applications, highest sensitivity	Barié and Rapp[63], Kovacs and Venema[64], Brodie et al.[65], McHale[66]
Love waves	36° YX-cut LiNbO$_3$ and 64° YX-cut LiNbO$_3$	Very good accuracy in biosensing in a liquid environment	Highest sensitivity, limited applications in microfluidics	Brodie et al.[65], McHale[66]
R-waves	ST cut and Y-cut quartz, 128° Y-X-cut LiNbO$_3$ and X-112° Y-cut LiTaO$_3$	Streaming, Jetting, deformation, and nebulisation	Not ideal for liquid sensing	Fu et al.[13], Hess[48]
R-waves	AlN film SAWs	-	A good actuator as well as a good microfluidic heater	-
S-waves	ZnO with Aluminium plate	It can be used both for sensing and microfluidics. Gas sensing is double that of Rayleigh waves. These waves can be used for liquid pumping	Appear in thin-films only (when its velocity is lower than substrate)	Sezawa and Kanai[49], Hadj-Larbi and Serhane[67]
Hybridised waves	Al foil with ZnO as the top layer	The rate of nebulisation is increased at higher vibrational velocity	Vibration modes vary with structures	Liu et al.[38]

applications.[59] Optimal properties of the waves can be achieved by using normalised thickness ratio of piezo-electric film thickness (h) with the wavelength (λ) as $h_{ZnO}/\lambda = 0.304$.[60]

Table 1 summarises the classification of the waves, material required to generate those waves, applications of waves, and their problems/limitations.

Kinetic impacts have been elucidated in this section, how the waves change internal energy or temperature of the droplet has been explained in the following section.

Thermal impact of *SAW* on microdroplet

The SAW gives rise to the heating of liquid droplets and the underlying substrate[68–70] and is especially critical at high RF input power.[71] There can be two reasons for heating of the droplet: propagation of the waves inside the substrate induces mechanical vibrations and stresses which causes acoustic heating; the generated heat is then conducted into the liquid droplet. Second reason of heating is energy dissipation of longitudinal waves inside the droplet due to viscous friction that causes convection. The latter phenomenon dominates the heating process and increases the temperature of the droplet.[22,72]

Heating mechanism of microdroplet

The temperature rise of the droplet (T_d) is a joint result of acousto-thermal effect and Joule heat effect.[73] Whereas Joule heat effect can be defined as, production of heat by passing electric current through the conductor. Droplet heating using joule-heat effect (without acoustic waves) gives 26°C temperature rise. While application of Gold (Au) layer as a shield on electrode which bypasses an alternating current (AC), gives temperature of 34.50°C, that is temperature because of only acoustic waves. On the other hand, without a shield, joule-heat effect added with the acoustothermal
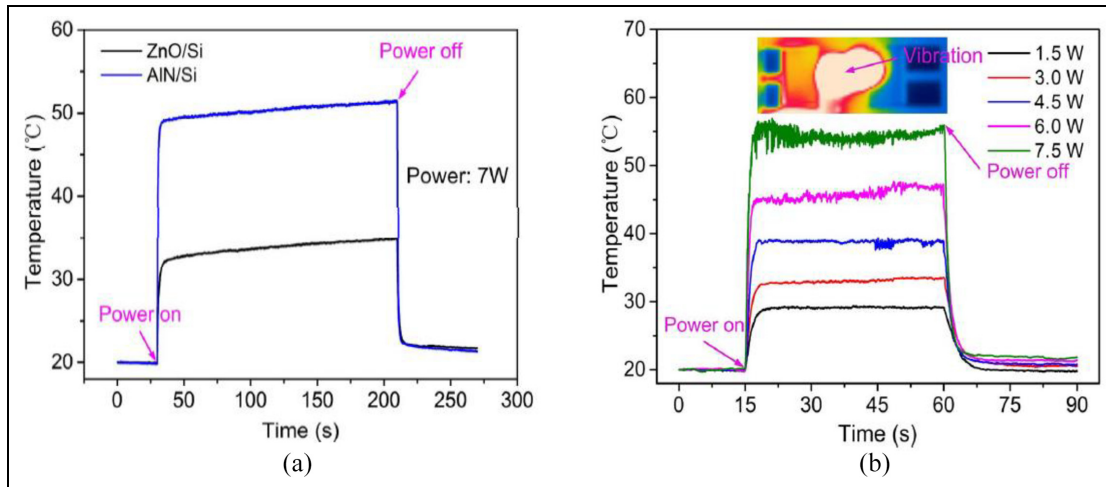
Figure 4. (a) Temperature of the droplet with ZnO/Si and AlN/Si devices and (b) temperature of the droplet at different input power levels using an Aluminium plate as a substrate.[75]

effect to give temperature rise of 43.50°C.[73] Other than Joule-heat, convection (streaming) and viscous dissipation inside the droplet plays a significant role in the temperature rise of the droplet. On the other hand, the droplet's temperature is 1.5 times more as compared to the substrate's temperature when using the same input power and the substrate.[22] Similarly, T_d is double the temperature of the substrate when using the same input voltage (35 $V_{p\text{-}p}$) and same duty factor (50%).[68]

When impact of the substrate on the temperature change of the microdroplet was evaluated, LiNbO$_3$ revealed a five-fold increase in temperature when compared to the ST-X (cut direction) quartz substrate mainly due to the low electromechanical coupling coefficient of quartz.[74] A comparison of acoustic heating of the substrate (without droplet) using ZnO/Si and AlN/Si showed that AlN/Si exhibit better acoustic heating performance as shown in Figure 4(a). This can be due to the lower electromechanical coupling coefficient of AlN/Si which results in better power conversion to heat.[75] Furthermore, the temperature of the droplet is directly related to the amount of energy it receives that corresponds to larger vibrations, shown in Figure 4(b). As temperature stability is difficult to achieve using water droplets, a PDMS chamber is used so that the temperature can be controlled digitally and thermal stability is achieved using SAW heating.[75]

The Peclet number ($Pe = \frac{\rho.c.v.L}{k}$), which relates thermal convection to conduction, gives a better understanding of the heat transfer process inside the droplet; here ρ is density (kg/m^3), c is the heat capacity (J.kg^{-1}.K^{-1}), v is the streaming velocity (m.s^{-1}), L is the characteristic length (m) and k is thermal conductivity (W.m^{-1}.K^{-1}) of the liquid.[76] At lower input power (100 mW), steaming velocity will be less ($Pe \ll 1$), therefore there will be conduction heat transfer.

However, at the higher power (1.6 W), streaming velocity will be higher ($Pe \gg 1$), so convection will dominate that increases the heat inside the droplet. On the other hand, if the viscosity of the liquid droplet increases, this will reduce the streaming velocity due to frictional impacts, therefore making conduction more dominant in heat transfer. As a result, longer time scales are required to reach the thermal equilibrium.[76,77] High viscous fluids exhibit larger resistance to heat dissipation, therefore, shows a substantial temperature rise compared to those of lower viscosities.

When comparing the impact of the resonant frequency on the temperature rise of the droplet for both water and glycerol droplets, lower frequency displayed a larger temperature change compared to higher frequencies.[72] This may be because higher frequencies have more attenuation and most of the energy decays in the substrate while transferring to the droplet.

It is important to understand the impact of SAW radiation inside the droplet after waves immediately enter inside the droplet. In a recently conducted study,[69] the temperature rise (T_d) was measured from both sides of the droplet, that is, SAW entering side as well as on opposite side of the droplet which is away from the IDT. T_d near the side where the waves enter was found 5% higher than the other side after 80 s of SAW acting time.

Temperature uniformity inside microdroplet

The change in resonant frequency, RF power of the SAW and change in volume of the droplet have an impact on temperature uniformity of the droplet.[77] IDTs can be fabricated by different methods that define their fundamental harmonic resonant frequency. Therefore, IDTs have different resonant frequencies to
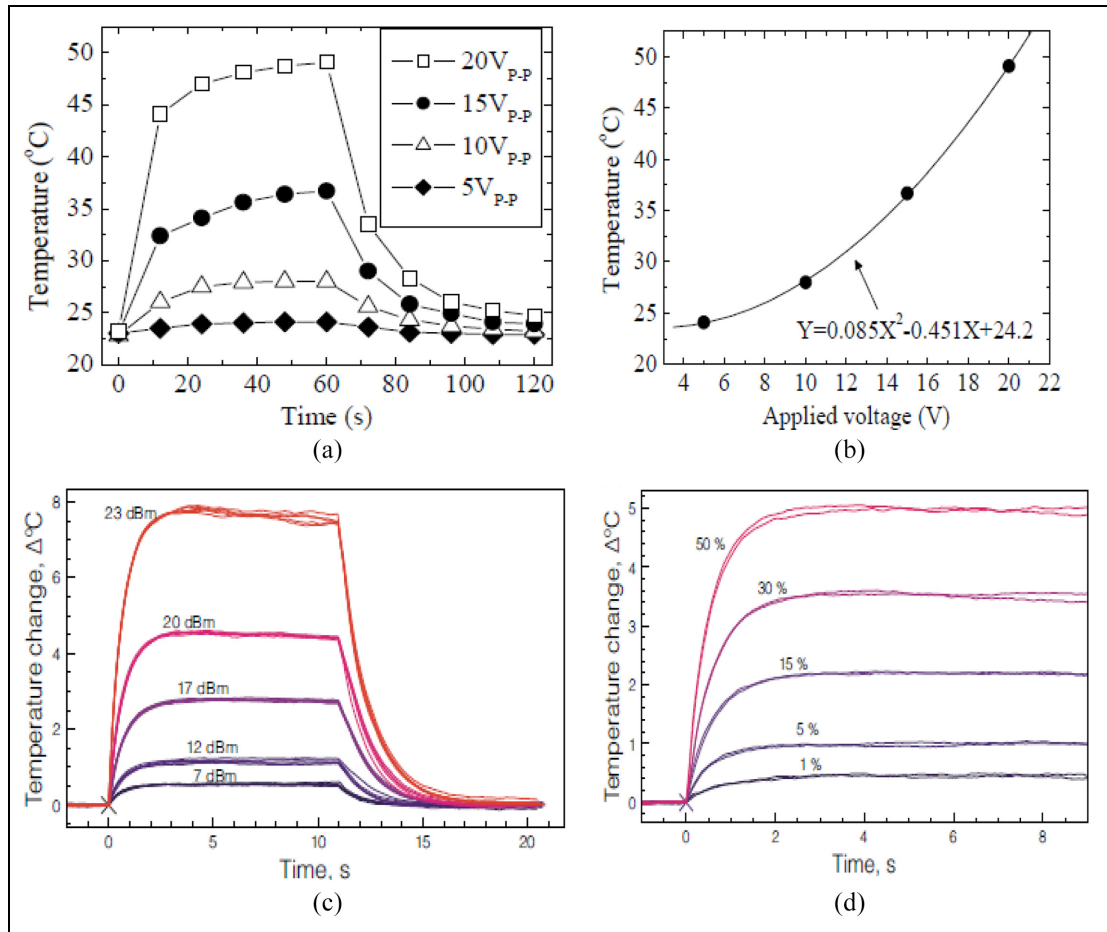
Figure 5. Experimental results showing impact of input voltage or power on the temperature of the droplet (a) temperature of a 10 μl water droplet versus time at different input voltages, (b) temperature achieved after 1 min of applying different voltages,[68] (c) change in temperature of the droplet at different input powers to the device, and (d) change in temperature by changing the duty cycle at constant input power of 23 dBm.[24]

achieve maximum acoustic efficiency. Moreover, temperature of the substrate material also affects the resonant frequency which in turn change the temperature uniformity inside the microdroplet.[20,78] In addition, damping of the Rayleigh SAW in the piezoelectric substrate called attenuation also plays an important role in gaining temperature uniformity of the droplet.[7] Attenuation is enhanced at higher resonant frequency of the input wave due to which it takes more time to reach thermal equilibrium. Moreover, attenuation of the waves is directly related to the volume of the droplet and input RF power.[77] It is important to note that microfluidics heating systems based on the SAW experience forced convection whereas other heating systems involve conduction only. Therefore, SAW based heating system have higher temperature uniformity inside the droplet.

The temperature rise of the droplet can be controlled by changing the duty factor or changing the input voltage/power.[68] The change in temperature of a 10 μl droplet at different input peak to peak voltages (5 V_{p-p}, 10 V_{p-p}, 15 V_{p-p} and 20 V_{p-p}) applied for 2 min, is presented in Figure 5(a).[68] The trend shows exponential relation between an input voltage and temperature change of the droplet as shown in Figure 5(b). Furthermore, amplitude of the SAW has direct relation to applied voltage,[79,80] therefore the temperature change is directly proportional to the square of SAW amplitude that directly corresponds to changes in the streaming force.[81] Both heating and cooling can be done by either changing the input power (dBm/Watt) or changing the duty cycle (%) as illustrated in Figure 5(c) and (d).[24] The microdroplet reaches the steady-state within 2.0 s of the SAW input time.

Heating of the droplet is insignificant when the input power is less than 0.50 W. However, this starts dominating when the input power is more than 0.50 W. Rise
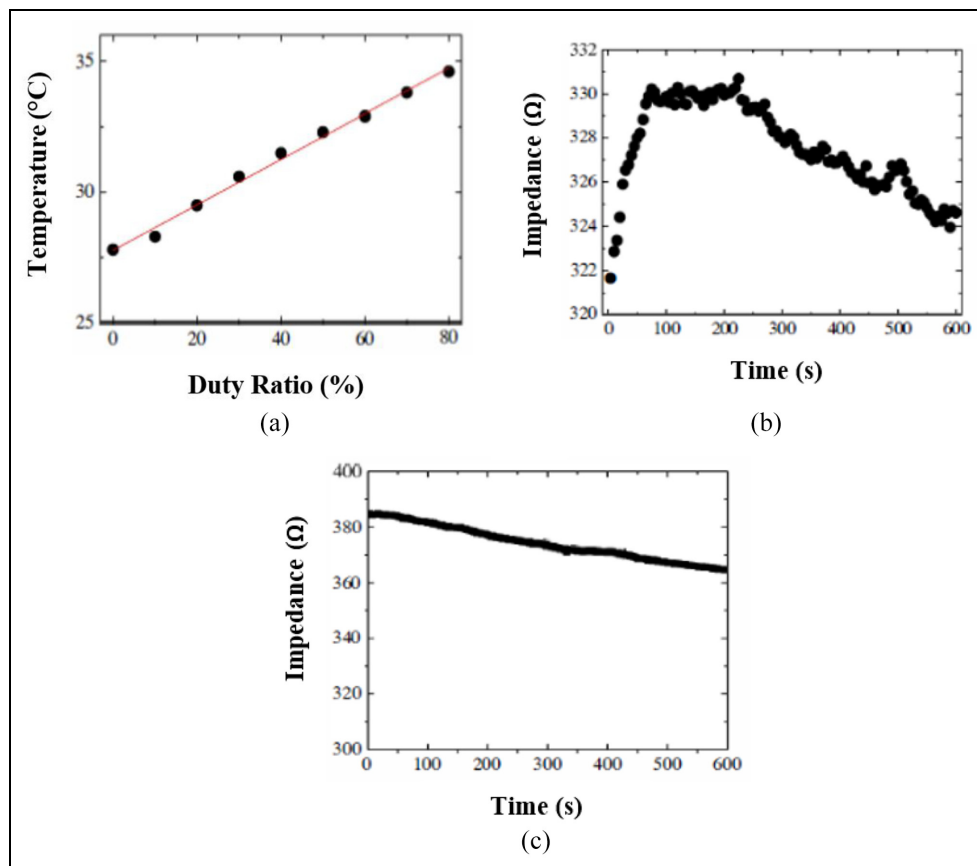
Figure 6. (a) Effect of duty ratio on temperature after 60 s of applied power (1.0 W), (b) change in impedance versus time with SAW during coagulation reaction, and (c) change in impedance versus time without temperature control by SAW.[97]

in temperature of the droplet has been observed to be 20°C when the input power is 2.0 W. There is a direct relation between streaming velocity and rise in temperature of the droplet. Convection helps in obtaining uniform temperature inside the droplet.

Applications of surface acoustic waves in the medical industry

Applications of the acoustic waves are not limited to but are widely in use for different medical diagnostics including elasticity imaging,[82–85] targeted imaging and therapy,[86–88] pulmonary drug delivery,[89] as an acoustic tweezer,[90,91] Polymerase Chain Reaction and Thermocycler.

Pulmonary drug delivery

Nebulisation has been widely used in the drug delivery and transportation of droplets. It has been a challenge to generate droplets of size sub-microns for targeted lung area but with the help of SAW devices, microdroplets have been produced and are widely available in the literature.[25,92–94]

Monitoring blood clotting

Controlled temperature is required to change in impedance of the blood samples can be used to diagnose clotting in the blood.[95,96] Ohashin and Kondoh[97] used Lamb waves with a centre frequency of 50.6 MHz at an input power of 1.0 W for this purpose. An activated partial thromboplastin time (APTT) plasma and calcium chloride sample solution (5 μl) was used for testing during the experiment. The electrical impedance of the blood sample was measured at a constant temperature of 37°C. SAW was used to maintain this temperature using duty cycle. A linear relation between duty ratio and temperature rise was found as shown in Figure 6(a). A significant change in impedance with time can be clearly seen in Figure 6(b) which illustrates variation in impedance with time when temperature of the sample was kept constant at 37°C. However, there is not much change in the impedance in the absence of SAW as depicted in Figure 6(c). A change in impedance shows clotting in the blood sample, however, this wasn't possible without using SAW. Therefore, these results show that SAW is helpful in monitoring the blood clotting.

Lamb waves employing FPWs generated by Si/SiO$_2$/Si$_3$N$_4$/Cr/Au/ZnO based devices have successfully been applied to observe concentration of immunoglobulin E (IgE) in the human blood.[98] Furthermore, the SSAW can also be used to separate platelets from whole blood.[99]

Acoustic tweezer

Another important application of SAW in the medical industry is an acoustic tweezer that can be used for droplet sorting or microparticle trapping.[100,101] With the centre frequency of 70–95 MHz with LiNbO$_3$ as a substrate and PDMS channel using variable input signal, droplets can be sorted out using the temperature gradient. Because of acoustothermal heating, the droplet can move from a higher temperature area to a lower temperature area.[100]

There are certain applications where controlled temperature is required for constant heating or cooling phases. SAW can also be efficiently used for certain applications where the variable temperature is required.

Polymerase chain reaction and thermocycler

Polymerase Chain Reaction (PCR) is an important process that is currently being used in many applications including detecting SARS-CoV-2 from suspected COVID-19 patients.[102] PCR is also called a thermocycler in which controlled temperature of the liquid is a key requirement.[103] As discussed earlier, the temperature of the fluids can be controlled by adjusting different parameters including applied voltage, duty ratio, and viscosity of the fluid.[104] For reactions like PCR, we need to achieve temperature of around 100°C. Water can not be heated above 50°C during the test. However, we can achieve a temperature of 50°C, 72°C, 98°C and 120°C with 80% water/glycerol mixture and duty factor of 20%, 40%, 60% and 80% respectively.[104] PCR is a tool to amplify DNA samples that is useful for virus identification, DNA genotyping, and forensic applications.[105,106] The PCR is a low-cost test and have an increased ramp rate with homogeneous temperature equilibrium. Microfluidic heat exchangers have been used to achieve accelerated heating (44°C/s) and cooling (17°C/s) which helped to augment DNA/RNA of H5N1 influenza, a human immunodeficiency virus (HIV).[107] Rapid heating and cooling (100°C/s and 90°C/s) can also be achieved using a Peltier junction along with a thermocouple[108] but SAW based heating and cooling cycles are more efficient for PCR applications.[109] As PCR requires continuous heating and cooling cycles that can be achieved by changing the duty cycle using SAW.[109]

High viscous fluids have conduction heat transfer due to close proximity of molecules. In addition, there
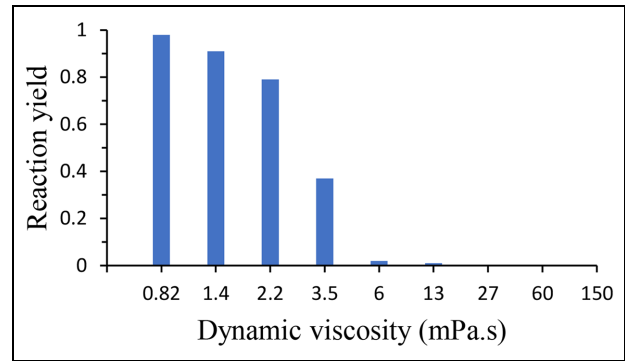

Figure 7. Variation in PCR reaction yield of a common industrial thermocycler as a function of viscosity of liquid.[110]

is a challenge to interact species with each other using high viscous liquids. Efficiency of the reaction (PCR) decreases dramatically when the absolute viscosity attains the value of 3.5 MPa s, as illustrated in Figure 7.[110] However, Rayleigh surface acoustic waves promotes convection. As discussed in section 3.1, streaming velocity inside the droplet is more due to convection heat transfer which enhances internal mixing, hence improves PCR efficiency even using high viscous fluids.[76,110] Moreover, it is important to note that the PCR mixture is unaffected by the wave's power or duration of irradiation, indicating that R-SAW is compatible with microdroplet PCR.[110]

Conclusions and recommendations

In this article, kinetic and thermal impacts of the surface acoustic waves on the microlitre droplets are reviewed. The classification of acoustic waves based on different types of IDTs are analysed followed by discussion of their applications in relevant medical fields. It is determined that the standard IDTs are good for both sensing and microfluidic applications while bendable IDTs are beneficial for medical sensing, wearable diagnostics, and surgical instruments. Circular IDTs are suitable for mixing, pumping while F-IDTs are useful for jetting, deformation, and heating of the droplet. It is observed that BAW-FBAR, Love waves, and S-waves are feasible for sensing applications while Lamb waves can be used both for sensing and microfluidics applications. R-SAW are good for microfluidics applications while SSAWs are ideal for particle separation, manipulation, and patterning. Moreover, standard IDTs, circular and focussed IDTs can be used for heating applications.

There are two reasons for heating of the droplet. One is heat transfer from substrate to the droplet and other is due to wave propagation inside the droplet. LiNbO$_3$ exhibits better performance in terms of

convection heat transfer inside droplet as compared to ST X quartz. SAW can be used as an acoustic tweezer and is an efficient tool to monitor blood clotting that is important for cardiovascular, and liver-related diseases. These waves can be employed for pulmonary drug delivery, monitoring concentration of immunoglobulin (lgE) in the human blood. Moreover, SAW can be effectively utilised to control the droplet's temperature by either using the duty cycle or by varying the input power. Furthermore, the waves can be the means to get the uniform temperature inside the droplet and can be successfully employed for applications like PCR.

SH-SAW and Love waves have high sensitivity making them unsuitable for microfluidic applications. Love waves are especially good for biosensing in the liquid environment. SSAWs are good for particles separation, cell sorting, cell patterning but are only limited to channel-based microfluidics, not good for droplet-based microfluidics. R-waves are good both for the inside droplet kinetics and jetting, nebulisation of the droplet. It is experimentally proved that R-waves can be efficiently used as a microfluidic heater and can also be used for PCR applications.

This article mainly focussed on experimental investigations related to droplet-based acoustofluidics using deionised water droplets. It can also serve as the basis for PDMS channel-based fluids with different viscosities where the thermal impact of the convection inside the liquid can be analysed to benefit the community.

Declaration of conflicting interests

The author(s) declared no potential conflicts of interest with respect to the research, authorship, and/or publication of this article.

Funding

ORCID iDs

Javed Akhter https://orcid.org/0000-0003-2477-832X
Tariq Nawaz Chaudhary https://orcid.org/0000-0003-2695-4585

References

1. Delsing P, Cleland AN, Schuetz MJA, et al. The 2019 surface acoustic waves roadmap. *J Phys D Appl Phys* 2019; 52: 353001.
2. Campanella H, Esteve J, Montserrat J, et al. Localized and distributed mass detectors with high sensitivity based on thin-film bulk acoustic resonators. *Appl Phys Lett* 2006; 89: 033507.
3. Lakin KM. Thin film resonator technology. In: *IEEE International frequency control symposium and PDA exhibition jointly with the 17th European frequency and time forum*, 2003, 2003, pp.765–778. New York, NY: IEEE.
4. Du J, Harding GL, Collings AF, et al. An experimental study of love-wave acoustic sensors operating in liquids. *Sens Actuators A Phys* 1997; 60: 54–61.
5. Rocha-Gaso M-I, March-Iborra C, Montoya-Baides A, et al. Surface generated acoustic wave biosensors for the detection of pathogens: a review. *Sensors* 2009; 9: 5740–5769.
6. Thurston RN, Pierce AD and Papadakis EP. *Reference for modern instrumentation, techniques, and technology: Ultrasonic instruments and devices I: Ultrasonic instruments and devices I*. London: Academic Press, 1998.
7. Connacher W, Zhang N, Huang A, et al. Micro/nano acoustofluidics: materials, phenomena, design, devices, and applications. *Lab Chip* 2018; 18: 1952–1996.
8. Hartmann CS. Systems impact of modern Rayleigh wave technology. In: Ash EA and Paige EGS (eds) *Rayleigh-wave theory and application*. Berlin, Heidelberg: Springer, 1985, 238–253.
9. Zhou C, Yang Y, Zhan J, et al. Surface acoustic wave characteristics based on c-axis (006) LiNbO3/diamond/silicon layered structure. *Appl Phys Lett* 2011; 99: 022109.
10. Chen J, Zhang Q, Han T, et al. Theoretical analysis of surface acoustic wave propagating properties of Y-cut nano lithium niobate film on silicon dioxide. *AIP Adv* 2015; 5: 087173.
11. Kadota M, Ogami T, Yamamoto K, et al. High-frequency lamb wave device composed of MEMS structure using LiNbO3 thin film and air gap. *IEEE Trans Ultrason Ferroelectr Freq Control* 2010; 57: 2564–2571.
12. Lam HK, Dai JY and Chan HL. Orientation controllable deposition of LiNbO3 films on sapphire and diamond substrates for surface acoustic wave device application. *J Cryst Growth* 2004; 268: 144–148.
13. Fu YQ, Luo JK, Nguyen N-T, et al. Advances in piezoelectric thin films for acoustic biosensors, acoustofluidics and lab-on-chip applications. *Prog Mater Sci* 2017; 89: 31–91.
14. Wixforth A, Strobl C, Gauer CH, et al. Acoustic manipulation of small droplets. *Anal Bioanal Chem* 2004; 379: 982–991.
15. Sritharan K, Strobl CJ, Schneider MF, et al. Acoustic mixing at low Reynold's numbers. *Appl Phys Lett* 2006; 88: 054102.
16. Du XY, Swanwick ME, Fu YQ, et al. Surface acoustic wave induced streaming and pumping in 128° Y-cut LiNbO$_3$ for microfluidic applications. *J Micromech Microeng* 2009; 19: 35016.
17. Zhou J, Tao X, Luo J, et al. Nebulization using ZnO/Si surface acoustic wave devices with focused interdigitated transducers. *Surf Coat Technol* 2019; 367: 127–134.
18. Yeo LY, Friend JR, McIntosh MP, et al. Ultrasonic nebulization platforms for pulmonary drug delivery. *Expert Opin Drug Deliv* 2010; 7: 663–679.

19. Fu YQ, Li Y, Zhao C, et al. Surface acoustic wave nebulization on nanocrystalline ZnO film. *Appl Phys Lett* 2012; 101: 194101.

20. Ha BH, Lee KS, Destgeer G, et al. Acoustothermal heating of polydimethylsiloxane microfluidic system. *Sci Rep* 2015; 5: 11851.

21. Kondoh J, Shimizu N, Matsui Y, et al. Liquid heating effects by SAW streaming on the piezoelectric substrate. *IEEE Trans Ultrason Ferroelectr Freq Control* 2005; 52: 1881–1883.

22. Beyssen D, Le Brizoual L, Elmazria O, et al. 6I-2 Droplet heating system based on SAW/liquid interaction. In: *2006 IEEE ultrasonics symposium*, 2006, pp.949–952. New York, NY: IEEE.

23. Das PK, Snider AD and Bhethanabotla VR. Acoustothermal heating in surface acoustic wave driven microchannel flow. *Phys Fluids* 2019; 31: 106106.

24. Shilton RJ, Mattoli V, Travagliati M, et al. Rapid and controllable digital microfluidic heating by surface acoustic waves. *Adv Funct Mater* 2015; 25: 5895–5901.

25. Qi A, Friend JR, Yeo LY, et al. Miniature inhalation therapy platform using surface acoustic wave microfluidic atomization. *Lab Chip* 2009; 9: 2184–2193.

26. Qi A, Yeo L, Friend J, et al. The extraction of liquid, protein molecules and yeast cells from paper through surface acoustic wave atomization. *Lab Chip* 2010; 10: 470–476.

27. Rezk AR, Tan JK and Yeo LY. HYbriD resonant acoustics (HYDRA). *Adv Mater Weinheim* 2016; 28: 1970–1975.

28. White RM and Voltmer FW. Direct piezoelectric coupling to surface elastic waves. *Appl Phys Lett* 1965; 7: 314–316.

29. Darmawan M and Byun D. Focused surface acoustic wave induced jet formation on superhydrophobic surfaces. *Microfluid Nanofluidics* 2015; 18: 1107–1114.

30. de Lima MM, Alsina F, Seidel W, et al. Focusing of surface-acoustic-wave fields on (100) GaAs surfaces. *J Appl Phys* 2003; 94: 7848–7855.

31. Wu TT and Chang I-H. Actuating and detecting of microdroplet using slanted finger interdigital transducers. *J Appl Phys* 2005; 98: 024903.

32. Kim DL, Jeong WH, Kim GH, et al. Solution-processed indium–zinc oxide with carrier-suppressing additives. *J Inf Disp* 2012; 13: 113–118.

33. Sun Y and Rogers J. Inorganic semiconductors for flexible electronics. *Adv Mater Weinheim* 2007; 19: 1897–1916.

34. Zhou L, Wanga A, Wu SC, et al. All-organic active matrix flexible display. *Appl Phys Lett* 2006; 88: 083502.

35. Focke M, Kosse D, Müller C, et al. Lab-on-a-Foil: microfluidics on thin and flexible films. *Lab Chip* 2010; 10: 1365–1386.

36. Son D, Lee J, Qiao S, et al. Multifunctional wearable devices for diagnosis and therapy of movement disorders. *Nat Nanotechnol* 2014; 9: 397–404.

37. He X, Guo H, Chen J, et al. Bendable ZnO thin film surface acoustic wave devices on polyethylene terephthalate substrate. *Appl Phys Lett* 2014; 104: 213504.

38. Liu Y, Li Y, el-Hady AM, et al. Flexible and bendable acoustofluidics based on ZnO film coated aluminium foil. *Sens Actuators B Chem* 2015; 221: 230–235.

39. Jangi M, Luo JT, Tao R, et al. Concentrated vertical jetting mechanism for isotropically focused zno/Si surface acoustic waves. *Int J Multiphase Flow* 2019; 114: 1–8.

40. Alghane M, Fu YQ, Chen BX, et al. Scaling effects on flow hydrodynamics of confined microdroplets induced by Rayleigh surface acoustic wave. *Microfluid Nanofluidics* 2012; 13: 919–927.

41. Fu YQ, Garcia-Gancedo L, Pang HF, et al. Microfluidics based on zno/nanocrystalline diamond surface acoustic wave devices. *Biomicrofluidics* 2012; 6: 24105–2410511.

42. Fu YQ, Luo JK, Du XY, et al. Recent developments on ZnO films for acoustic wave based bio-sensing and microfluidic applications: a review. *Sens Actuators B Chem* 2010; 143: 606–619.

43. Dung Luong T and Trung Nguyen N. Surface Acoustic Wave Driven Microfluidics – A review. *Micro Nanosystems* 2010; 2: 217–225.

44. Nguyen EP, Lee L, Rezk AR, et al. Hybrid surface and bulk resonant acoustics for concurrent actuation and sensing on a single microfluidic device. *Anal Chem* 2018; 90: 5335–5342.

45. Wang Y, Tao X, Tao R, et al. Acoustofluidics along inclined surfaces based on AlN/Si Rayleigh surface acoustic waves. *Sens Actuators A Phys* 2020; 306: 111967.

46. Cheng CC, Lin RC, Chang WT, et al. Electromechanical coupling coefficient of SAW on proton-exchanged and annealed LiNbO$_3$ Waveguides. *Adv Mater Res* 2011; 311–313: 1957–1960.

47. Singh R, Sankaranarayanan SKRS and Bhethanabotla VR. Enhanced surface acoustic wave biosensor performance via delay path modifications in mutually interacting multidirectional transducer configuration: A computational study. *Appl Phys Lett* 2009; 95: 034101.

48. Hess P. Surface acoustic waves in materials science. *Phys Today* 2002; 55: 42–47.

49. Sezawa K and Kanai K. Discontinuity in dispersion curves of Rayleigh-waves. *Proc Imp Acad* 1935; 11: 13–14.

50. Muller A, Giangu I, Stavrinidis A, et al. Sezawa propagation mode in GaN on Si surface acoustic wave type temperature sensor structures operating at GHz frequencies. *IEEE Electron Device Lett* 2015; 36: 1299–1302.

51. Mehmood M. *Experimental investigation of thermal and kinetic impacts of surface acoustic waves on water droplet.* PhD Thesis, Heriot-Watt University, Edinburgh, 2020.

52. Pepper J, Noring R, Klempner M, et al. Detection of proteins and intact microorganisms using microfabricated flexural plate silicon resonator arrays. *Sens Actuators B Chem* 2003; 96: 565–575.

53. Roy Mahapatra D, Singhal A and Gopalakrishnan S. Lamb wave characteristics of thickness-graded piezoelectric IDT. *Ultrasonics* 2005; 43: 736–746.

54. Grate JW, Wenzel SW and White RM. Frequency-independent and frequency-dependent polymer transitions observed on flexural plate wave ultrasonic sensors. *Anal Chem* 1992; 64: 413–423.

55. Moroney RM, White RM and Howe RT. Microtransport induced by ultrasonic Lamb waves. *Appl Phys Lett* 1991; 59: 774–776.

56. Pyun JC, Beutel H, Meyer J-U, et al. Development of a biosensor for E. Coli based on a flexural plate wave (FPW) transducer. *Biosens Bioelectron* 1998; 13: 839–845.

57. Shi J, Mao X, Ahmed D, et al. Focusing microparticles in a microfluidic channel with standing surface acoustic waves (SSAW). *Lab Chip* 2008; 8: 221–223.

58. Yeo LY and Friend JR. Surface acoustic wave microfluidics. *Annu Rev Fluid Mech* 2014; 46: 379–406.

59. Josse F, Bender F and Cernose RW. Guided shear horizontal surface acoustic wave sensors for chemical and biochemical detection in liquids. *Anal Chem* 2001; 73: 5937–5944.

60. Luo J-T, Quan A-J, Liang G-X, et al. Love-mode surface acoustic wave devices based on multilayers of TeO2/znoo(12⁻0)/Si(100) with high sensitivity and temperature stability.. *Ultrasonics* 2017; 75: 63–70.

61. Lamb H. On waves in an elastic plate. *Proc R Soc Lond A Math Phys Sci* 1917; 93: 114–128.

62. Muralt P, Ledermann N, Baborowski J, et al. Piezoelectric micromachined ultrasonic transducers based on PZT thin films. *IEEE Trans Ultrason Ferroelectr Freq Control* 2005; 52: 2276–2288.

63. Barié N and Rapp M. Covalent bound sensing layers on surface acoustic wave (SAW) biosensors. *Biosens Bioelectron* 2001; 16: 979–987.

64. Kovacs G and Venema A. Theoretical comparison of sensitivities of acoustic shear wave modes for (bio)chemical sensing in liquids. *Appl Phys Lett* 1992; 61: 639–641.

65. Brodie DS, Fu YQ, Li Y, et al. Shear horizontal surface acoustic wave induced microfluidic flow. *Appl Phys Lett* 2011; 99: 153704.

66. McHale G. Generalized concept of shear horizontal acoustic plate mode and Love wave sensors. *Meas Sci Technol* 2003; 14: 1847–1853.

67. Hadj-Larbi F and Serhane R. Sezawa SAW devices: review of numerical-experimental studies and recent applications. *Sens Actuators A Phys* 2019; 292: 169–197.

68. Kondoh J, Shimizu N, Matsui Y, et al. Development of temperature-control system for liquid droplet using surface acoustic wave devices. *Sens Actuators A Phys* 2009; 149: 292–297.

69. Ito S, Sugimoto M, Matsui Y, et al. Study of surface acoustic wave streaming phenomenon based on temperature measurement and observation of streaming in liquids. *Jpn J Appl Phys* 2007; 46: 4718–4722.

70. Renaudin A, Chabot V, Grondin E, et al. Integrated active mixing and biosensing using surface acoustic waves (SAW) and surface plasmon resonance (SPR) on a common substrate. *Lab Chip* 2010; 10: 111–115.

71. Greco G, Agostini M, Shilton R, et al. Surface Acoustic Wave (SAW)-Enhanced chemical functionalization of Gold Films. *Sensors* 2017; 17: 2452.

72. Huang Q-Y, Sun Q, Hu H, et al. Thermal effect in the process of surface acoustic wave atomization. *Exp Therm Fluid Sci* 2021; 120: 110257.

73. Zheng T, Wang C, Hu Q, et al. The role of electric field in microfluidic heating induced by standing surface acoustic waves. *Appl Phys Lett* 2018; 112: 233702.

74. Li S, Desrosiers J and Bhethanabotla VR. Heating of Rayleigh surface acoustic wave devices in 128° YX LiNbO 3 and ST X quartz substrates. In: *2017 IEEE Sensors*, 2017, pp.1–3. New York, NY: IEEE.

75. Wang Y, Zhang Q, Chen D, et al. Rapid and controllable digital microfluidic heating using AlN/Si Rayleigh surface acoustic waves. In: *Proceedings of the IEEE international conference on micro electro mechanical systems (MEMS) 2020*, January 2020, pp.1098–1101. New York, NY: IEEE.

76. Beyssen D, Sarry F and Roux-Marchand T. Correlation of heat transfers mechanism(s) and time constant equilibrium on digital Rayleigh-saw microfluidic system. *Procedia Eng* 2015; 120: 1067–1070.

77. Roux-Marchand T, Beyssen D, Sarry F, et al. Rayleigh surface acoustic wave as an efficient heating system for biological reactions: investigation of microdroplet temperature uniformity. *IEEE Trans Ultrason Ferroelectr Freq Control* 2015; 62: 729–735.

78. Lee D, Lee N, Choi G, et al. Heat transfer characteristics of a focused surface acoustic wave (F-SAW) device for interfacial droplet jetting. *Inventions* 2018; 3: 38.

79. Sano A, Matsui Y and Shiokawa S. New manipulator based on surface acoustic wave streaming. *Jpn J Appl Phys* 1998; 37: 2979–2981.

80. Chono K, Shimizu N, Matsui Y, et al. Development of novel atomization system based on SAW streaming. *Jpn J Appl Phys* 2004; 43: 2987–2991.

81. Shiokawa S and Matsui Y. The dynamics of SAW streaming and its application to fluid devices. *MRS Online Proc Lib* 1994; 360: 53–64.

82. Fatemi M and Greenleaf JF. Vibro-acoustography: an imaging modality based on ultrasound-stimulated acoustic emission. *Proc Natl Acad Sci U S A* 1999; 96: 6603–6608.

83. Nightingale K, Soo MS, Nightingale R, et al. Acoustic radiation force impulse imaging: in vivo demonstration of clinical feasibility. *Ultrasound Med Biol* 2002; 28: 227–235.

84. Sarvazyan AP, Rudenko OV, Swanson SD, et al. Shear wave elasticity imaging: a new ultrasonic technology of medical diagnostics. *Ultrasound Med Biol* 1998; 24: 1419–1435.

85. Bercoff J, Tanter M and Fink M. Supersonic shear imaging: a new technique for soft tissue elasticity mapping. *IEEE Trans Ultrason Ferroelectr Freq Control* 2004; 51: 396–409.

86. Lizzi FL, Muratore R, Deng CX, et al. Radiation-force technique to monitor lesions during ultrasonic therapy. *Ultrasound Med Biol* 2003; 29: 1593–1605.

87. Bercoff J, Pernot M, Tanter M, et al. Monitoring thermally-induced lesions with supersonic shear imaging. *Ultrason Imaging* 2004; 26: 71–84.

88. Maleke C and Konofagou EE. Harmonic motion imaging for focused ultrasound (HMIFU): a fully integrated technique for sonication and monitoring of thermal ablation in tissues. *Phys Med Biol* 2008; 53: 1773–1793.

89. Dayton P, Klibanov A, Brandenburger G, et al. Acoustic radiation force in vivo: a mechanism to assist targeting of microbubbles. *Ultrasound Med Biol* 1999; 25: 1195–1201.

90. Santoso AK. A/spl pi/-shaped ultrasonic tweezers concept for manipulation of small particles. *IEEE Trans Ultrason Ferroelectr Freq Control* 2004; 51: 1499–1507.

91. Lee J, Ha K and Shung KK. A theoretical study of the feasibility of acoustical tweezers: Ray acoustics approach. *J Acoust Soc Am* 2005; 117: 3273–3280.

92. Heron SR, Wilson R, Shaffer SA, et al. Surface acoustic wave nebulization of peptides as a microfluidic interface for mass spectrometry. *Anal Chem* 2010; 82: 3985–3989.

93. Collins DJ, Manor O, Winkler A, et al. Atomization off thin water films generated by high-frequency substrate wave vibrations. *Phys Rev E* 2012; 86: 56312.

94. Rajapaksa A, Qi A, Yeo LY, et al. Enabling practical surface acoustic wave nebulizer drug delivery via amplitude modulation. *Lab Chip* 2014; 14: 1858–1865.

95. Berney H and O'riordan JJ. Impedance measurement monitors blood coagulation. *Analog Dialogue* 2008; 42: 8–42.

96. Ur A. Changes in the electrical impedance of blood during coagulation. *Nature* 1970; 226: 269–270.

97. Ohashin N and Kondoh J. Temperature control of a droplet on disposable type microfluidic system based on a surface acoustic wave device for blood coagulation monitoring. In: *Ultrasonics symposium (IUS), 2015 IEEE International*, 2015, pp.1–4. New York, NY: IEEE.

98. Huang I-Y and Lee M-C. Development of a FPW allergy biosensor for human IgE detection by MEMS and cystamine-based SAM technologies. *Sens Actuators B Chem* 2008; 132: 340–348.

99. Nam J, Lim H, Kim D, et al. Separation of platelets from whole blood using standing surface acoustic waves in a microchannel. *Lab Chip* 2011; 11: 3361–3364.

100. Park J, Jung JH, Destgeer G, et al. Acoustothermal tweezer for droplet sorting in a disposable microfluidic chip. *Lab Chip* 2017; 17: 1031–1040.

101. Silva GT and Baggio AL. Designing single-beam multi-trapping acoustical tweezers. *Ultrasonics* 2015; 56: 449–455.

102. Alteri C, Cento V, Antonello M, et al. Detection and quantification of SARS-CoV-2 by droplet digital PCR in real-time PCR negative nasopharyngeal swabs from suspected COVID-19 patients. *PLoS One* 2020; 15: e0236311.

103. Bell AS and Ranford-Cartwright LC. Real-time quantitative PCR in parasitology. *Trends Parasitol* 2002; 18: 337–342.

104. Kondoh J, Shimizu N, Matsui Y, et al. Development of SAW thermocycler for small liquid droplets. In: *IEEE Ultrasonics symposium*, 2005, 2005, pp.1023–1027. New York, NY: IEEE.

105. Mullis KB, Ferré F and Gibbs RA. *The polymerase chain reaction*. Boston: Binkhauser, 1994.

106. Adler MJ, Coronel C, Shelton E, et al. Increased gene expression of Alzheimer disease beta-amyloid precursor protein in senescent cultured fibroblasts. *Proc Natl Acad Sci U S A* 1991; 88: 16–20.

107. Maltezos G, Johnston M, Taganov K, et al. Exploring the limits of ultrafast polymerase chain reaction using liquid for thermal heat exchange: A proof of principle. *Appl Phys Lett* 2010; 97: 264101.

108. Maltezos G, Gomez A, Zhong J, et al. Microfluidic polymerase chain reaction. *Appl Phys Lett* 2008; 93: 243901.

109. Wheeler EK, Benett W, Stratton P, et al. Convectively driven polymerase chain reaction thermal cycler. *Anal Chem* 2004; 76: 4011–4016.

110. Roux-Marchand T, Beyssen D, Sarry F, et al. Rayleigh surface acoustic wave compatibility with microdroplet polymerase chain reaction. *Int J Microscale Nanoscale Therm Fluid Transp Phenom* 2013; 4: 231.

Appendix
Notation

Description	Symbol	Unit
The temperature rise of the droplet	T_d	(°C)
Wavelength	λ	μm
Thickness of substrate	h	μm
Activated partial thromboplastin time	APTT	
Flexural plate waves	FPW	
Interdigital transducer	IDT	
Lithium Niobate	$LiNbO_3$	
Lab-on-a-Chip	LOC	
Particle image velocimetery	PIV	
Polydimethylsiloxane	PDMS	
Lead Zirconate Titanate	PZT	
Polymerase Chain Reaction	PCR	
Radio Frequency	RF	
Rayleigh wave	R-wave	
Sezawa wave	S-wave	
Surface Acoustic Waves	SAW	
Standing Surface Acoustic Waves	SSAW	
Surface Generated Acoustic Waves	SGAW	
Surface Reflected Bulk Waves	SRBW	
Temperature co-efficient of frequency	TCF	
Zinc Oxide	ZnO	